Magnetic diffuse scattering of neutrons in an ordered Fe_3Pt Invar alloy

Yorihiko Tsunoda, Masao Takasaka, and Syusuke Hosoda
School of Science and Engineering, Waseda University, 3-4-1 Ohkubo, Shinjuku-ku, Tokyo 169-8555, Japan
(Received 21 May 2009; revised manuscript received 21 August 2009; published 8 October 2009)

Using an ordered $Fe_{72}Pt_{28}$ Invar alloy single-crystal, spin modulations due to the local lattice distortions in the premartensitic embryos were studied by neutron scattering. Magnetic diffuse scattering caused by the modulations of spin structure was found around the (1 0 0) and (1 1 0) super-lattice points. The diffuse scattering intensity caused by the spin modulations is far stronger than that due to the lattice displacement of the localized spins. The spin modulations extend to wider space than the cluster sizes with the lattice distortion. Relations are discussed between the spin modulations and the various anomalous magnetic behaviors reported by previous authors as common properties of the Invar alloys.

DOI: 10.1103/PhysRevB.80.134407 PACS number(s): 75.25.+z, 75.50.Bb, 61.05.F−, 81.30.Kf

I. INTRODUCTION

Very recently, present authors and colleague found existence of elastic diffuse scattering of neutrons around various Bragg-peak positions for FeNi Invar alloys as a premartensitic phenomenon of the fcc-bcc phase transition.[1] The diffuse scattering intensities depend on temperature and Ni concentration and increase with temperature decreasing and decrease with increasing Ni concentration. The diffuse scattering intensity pattern is different at each Bragg-peak position and is well explained by the formation of clusters with a lattice deformation described by a shear wave propagating along the ⟨1 1 0⟩ direction and the ⟨1−1 0⟩ polarization vector. The ranges of temperature and Ni concentration for which diffuse scattering is observed coincide with those for which the Invar anomalies are observable. Similar elastic diffuse scattering was also observed for other typical Invar alloys, ordered and disordered Fe_3Pt alloys. Thus, the appearance of clusters with a local lattice deformation described by a ⟨1 1 0⟩ shear wave seems to be closely related to the Invar effect.

On the other hand, magnetism of these systems has long been considered to play an important role to the Invar effect. Especially, the Weiss's 2-γ state model is considered to be the most accepted origin of the Invar effect.[2] With increasing temperature, Fe atoms of high-spin state with large atomic volume are excited to the low-spin state with small atomic volume. The loss of atomic volume in this process compensates the normal thermal expansion caused by the unharmonicity of the lattice potentials, resulting in a zero thermal-expansion coefficient. Various properties of Invar alloys reported before 1990 were summarized by Wasserman.[3] This paper reported anomalous magnetic behaviors as common properties of the Invar alloys. (1) Temperature variations in magnetization in low-temperature region decrease faster than those of ordinary ferromagnets with increasing temperature.[4] (2) High field susceptibilities do not saturate readily.[5] (3) Temperature variations in spin-wave stiffness D_{sw} determined by neutron inelastic scattering are not consistent with those estimated from the magnetization measurements.[6] (4) Spin-wave damping for the Invar alloys is very large comparing to those for ordinary ferromagnets.[7,8] These anomalous magnetic properties seem to be consistent with the Weiss's 2-γ state model[9] together with the many first-principles calculations for the Invar alloys.[10,11]

We can suspect that the local lattice deformation in the premartensitic embryos would have an influence to the magnetic structure of the Invar alloys. Purpose of the present experiments is to study the modulations of the spin structure caused by the lattice deformation using neutron scattering. Unfortunately, these typical Invar alloys are ferromagnet, indicating that in neutron-scattering experiments, magnetic scattering always overlaps on the nuclear scattering and the latter is far stronger than the former. To separate the magnetic scattering from the nuclear one, a polarized neutron technique is usually applied. We are now planning such an experiment. However, among these ferromagnetic alloys, an ordered Fe_3Pt alloy is a special case. An ordered Fe_3Pt alloy has an $L1_2$-type (Cu_3Au) structure as shown in Fig. 1 and the super-lattice reflections such as (1 0 0) and (1 1 0) are observed. These super-lattice reflections consist of both magnetic and nuclear components, and the peak intensities are proportional to the square of the differences of the scattering amplitudes in the alternate planes. However, the nuclear super-lattice peak intensities are negligibly small for an ordered Fe_3Pt alloy because the difference in nuclear scattering amplitudes of constituent elements happens to be almost zero ($b_{Fe}=9.45$ and $b_{Pt}=9.60\times10^{-13}$ cm). While, since there exists large difference between the sizes of magnetic moments of Fe and Pt ($m_{Fe}\approx2.8\ \mu_B$ and $m_{Pt}\approx0.8\ \mu_B$),[6] the magnetic super-lattice peak intensities are rather strong and the (1 0 0) and (1 1 0) super-lattice peaks are considered to be almost pure magnetic reflections. Thus, we can study the effect due

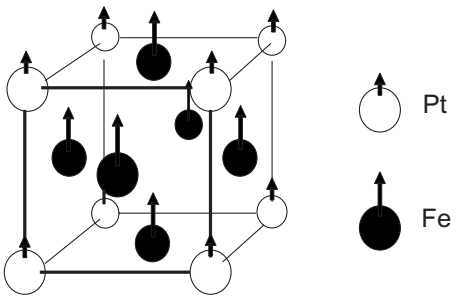

FIG. 1. Schematic illustration of atomic ($L1_2$-type) and magnetic structures of ordered Fe_3Pt alloy.

to the local lattice deformation on the magnetism of the Invar alloys through the magnetic super-lattice peaks of Fe_3Pt ordered alloy.

In this paper, we report that magnetic diffuse scattering was actually observed at these super-lattice positions and show that the diffuse scattering mainly arises from the modulations of spin structures due to the lattice deformations around the premartensitic embryos. Distribution of the magnetic diffuse scattering is confined to rather small **q** regions around the Bragg-peak positions. We discuss the spin modulations as a possible cause of the various anomalous magnetic properties observed common to the Invar alloys.

II. SAMPLE PREPARATION AND EXPERIMENTS

Since the stoichiometric Fe_3Pt alloy is too close to the phase boundary of an fcc-bcc martensitic transformation, $Fe_{75}Pt_{25}$ alloy is usually contaminated by a small portion of bcc phase even at room temperature. Thus, the off-stoichiometric alloy, $Fe_{72}Pt_{28}$ was used for the present experiments. Single crystal of $Fe_{72}Pt_{28}$ alloy was grown in an Al_2O_3 crucible using a furnace with a carbon electrode under an Ar gas atmosphere. To develop the $L1_2$-type atomic long-range order, the crystal was annealed at 1273 K for 48 h, then, the temperature was lowered 100 K every 24 h down to 373 K. Neutron scattering measurements were mainly performed at the T1–1 triple-axis spectrometer installed in the thermal guide of JRR-3M, Tokai. A part of the measurement was done at the T1–2 (AKANE) spectrometer. The incident neutron energies of 14.4 and 20 meV were used for the T1–1 and T1–2, respectively. To eliminate the higher order contamination, a thick pyrolitic graphite (PG) filter was set between the monochromator and the sample. All of the data were taken using a PG analyzer set to the elastic condition. The energy resolution for elastic incoherent peak was 0.66 meV for the T1–1 in the full width at the half maximum.

In Fig. 2(a), the observed super-lattice reflection at (1 0 0) is given. For comparison, that of a $Fe_{72}Pt_{28}$ disordered alloy is also given. For the disordered alloy, the crystal was quenched into water after annealing at 1273 K for 48 h. The disordered $Fe_{72}Pt_{28}$ alloy shows rather broad magnetic short-range order peak around (1 0 0) but the ordered sample showed a sharp Bragg peak at the (1 0 0) reciprocal-lattice point, indicating that the sample has sufficiently developed $L1_2$-type atomic order. In Fig. 2(b), a temperature variation in integrated intensity of the (1 0 0) peak for the ordered $Fe_{72}Pt_{28}$ alloy is given. These figures verify that the (1 0 0) peak is almost pure magnetic scattering and the Curie temperature of the present ordered sample is estimated to be 470 K.

III. EXPERIMENTAL DATA

To begin with, let us consider what is expected for the magnetic diffuse scattering when the spins couple with the local lattice deformations. If only the local lattice distortion exists but no spin modulations, and if we assume that the magnetic moments are localized at the atomic site, then, magnetic diffuse scattering with the same pattern as the

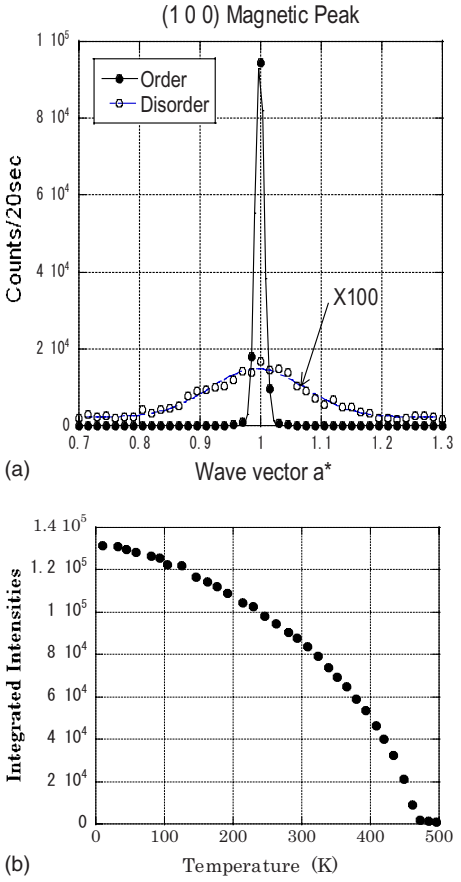

FIG. 2. (Color online) (a) The (1 0 0) super-lattice peak obtained for the ordered $Fe_{72}Pt_{28}$ alloy sample. For comparison, that of disordered alloy is also given with expanded scale (x 100). (b) Temperature variation in the integrated intensities of the (1 0 0) super-lattice peak.

nuclear diffuse scattering should be observed around the magnetic Bragg-peak positions because the nuclear scattering amplitude is simply replaced by the magnetic scattering amplitude. For instance, around the (1 0 0) magnetic Bragg-peak position, diffuse scattering with the same butterfly pattern as that around the (2 0 0) nuclear peak position should be observed (see Fig. 3). However, if the spin modulations coupled with the local lattice distortion exist, the diffuse scattering pattern changes.

Let us assume the lattice distortion described by a single wave with a wave vector **Q** for simplicity. The atomic position of the nth atom is described as

$$\mathbf{r_n} = \mathbf{na} + \mathbf{\Delta} \sin \mathbf{Qna}, \tag{1}$$

where Δ is an amplitude of the displacement wave. Then, the magnetic moment at the nth atom would be written as

$$\mathbf{S_n} = \mathbf{S}_0 + \delta\mathbf{S} \cos \mathbf{Qna} \tag{2}$$

because the spin modulation would have the maximum amplitude at the position with the maximum strain (not the maximum displacement). Where $\delta\mathbf{S}$ is an amplitude of the spin modulation wave. Substituting these values to the expression of the magnetic scattering intensity

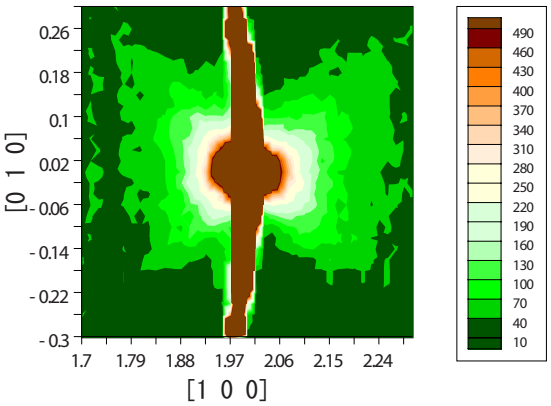

FIG. 3. (Color online) Intensity contour map of nuclear diffuse scattering obtained around the (2 0 0) Bragg-peak position at 10 K.

$$\mathbf{I}(\mathbf{K}) \propto |\mathbf{f}(\mathbf{K})|^2 \sum_{ij} \langle \mathbf{S_i S_j} \rangle \exp[\mathbf{iK}(\mathbf{r_i} - \mathbf{r_j})]\{1 - (\hat{\mathbf{k}} \cdot \hat{\mathbf{s}})^2\} \quad (3)$$

and neglecting the higher order terms, we obtain the scattering intensities at the first satellite peak positions as

$$\mathbf{I}(\tau \pm \mathbf{Q}) \propto |\mathbf{f}(\mathbf{K})|^2 \left(\frac{1}{4}\right)[(\mathbf{K} \cdot \mathbf{\Delta})\mathbf{S}_0^{\perp} \pm \delta\mathbf{S}^{\perp}]^2 \ \delta(\tau \pm \mathbf{Q})], \quad (4)$$

where $\mathbf{S_0^{\perp}}$ and $\delta\mathbf{S}^{\perp}$ are the perpendicular spin components to the scattering vector $\mathbf{K}$ and $f(\mathbf{K})$ indicates a magnetic form factor. The $(\mathbf{K}\cdot\mathbf{\Delta})\ \mathbf{S}_0^{\perp}$ term comes from the lattice displacement of localized spins and the $\delta\mathbf{S}^{\perp}$ term indicates the spin modulation due to the lattice deformation. From Eq. (4), if the $(\mathbf{K}\cdot\mathbf{\Delta})\ \mathbf{S}_0^{\perp}$ term and the $\delta\mathbf{S}^{\perp}$ term have the same order of magnitude, the satellite peak intensities of both sides become strongly asymmetric. The actual local lattice distortion would be described as the linear combination of the lattice waves with various wave vectors. Thus, the magnetic diffuse scattering intensities of both sides would become strongly asymmetric.

Prior to study the magnetic diffuse scattering, we checked that the $Fe_{72}Pt_{28}$ sample also shows nuclear diffuse scattering due to the lattice distortion as the premartensitic phenomena. Nuclear diffuse scattering with a typical butterfly pattern obtained at 10 K around the (2 0 0) reciprocal-lattice point is given in Fig. 3. The ridge extending along the [0 1 0] direction (the body of butterfly) comes from the mosaic spread of the single crystal. This pattern of diffuse scattering is very similar to that obtained for $Fe_{65}Ni_{35}$ alloy (see Fig. 1 of Ref. 1). The diffuse scattering includes the magnetic component because the $Fe_{72}Pt_{28}$ ordered alloy is a ferromagnet. However, the main contribution is nuclear scattering. As described in the previous paper, this pattern is well explained by the formation of clusters with the lattice deformation consisting of a shear wave propagating along the $\langle 1\ \ 1\ \ 0\rangle$ direction and with the $\langle 1 - 1\ \ 0\rangle$ polarization vector.

The intensity contour maps obtained around the (1 0 0) super-lattice point at 10, 300, and 484 K (1.03 T_c) are given in Fig. 4. These peaks are magnetic scattering as shown in Fig. 2(b). The circular pattern obtained above the Curie temperature (470 K) is ascribed to magnetic critical scattering. Below the Curie temperature, we can observe the side peaks extending along the $\langle 1\ \ 1\ \ 0\rangle$ direction only at the high scattering angle side and the side peak intensity increases with decreasing temperature. This peak looks to satisfy the condition described above, i.e., $(\mathbf{K}\cdot\mathbf{\Delta})\ \mathbf{S}_0^{\perp} \simeq \delta\mathbf{S}^{\perp}$ in the Eq. (4). However, since the line profile is rather sharp and the intensity is very high as diffuse scattering, we studied this peak using the T1–2 (AKANE) triple-axis spectrometer which is operated by a different incident neutron wavelength. Then, the peak disappeared as shown in Fig. 5, indicating that this peak is a spurious one and is considered to be multiple scattering in origin. The actual diffuse scattering due to the spin modulation is observed around the (1 0 0) Bragg-peak position. However, the observed diffuse scattering intensities of both sides are roughly symmetric, suggesting that either the relations $(\mathbf{K}\cdot\mathbf{\Delta})\ \mathbf{S}_0^{\perp} \gg \delta\mathbf{S}^{\perp}$ or the $\delta\mathbf{S}^{\perp} \gg (\mathbf{K}\cdot\mathbf{\Delta})\ \mathbf{S}_0^{\perp}$ is satisfied in the Eq. (4).

In order to determine which relations are realized for this system, we tried to estimate the term $|(\mathbf{K}\cdot\mathbf{\Delta})|^2$ from the in-

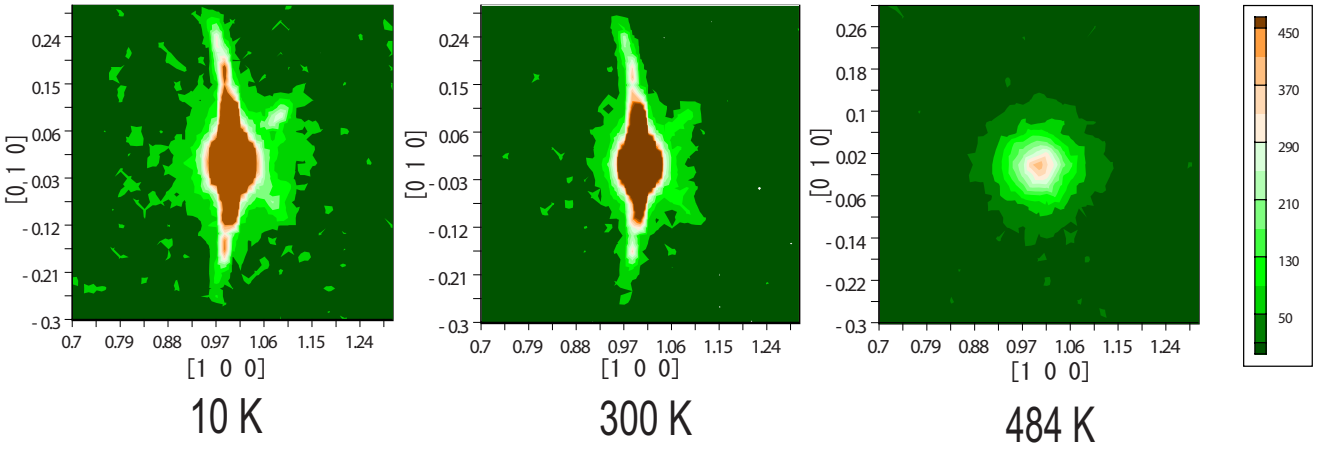

FIG. 4. (Color online) Intensity contour maps of magnetic diffuse scattering obtained around the (1 0 0) super-lattice position at 10, 300, and 484 K (1.03 T_c). The peaks at (1.09 ± 0.090) in the data below the Curie temperature are the spurious peak caused by multiple scattering (see text).

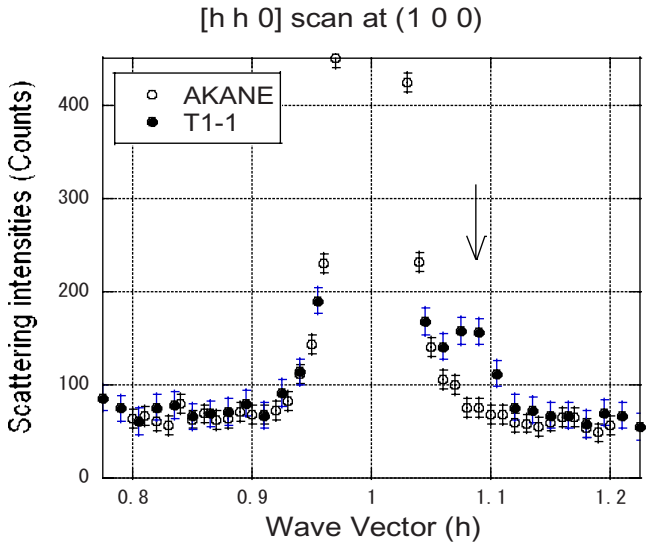

FIG. 5. (Color online) Line profiles obtained at room temperature by scanning along the [1 1 0] direction passing through the (1 0 0) reciprocal-lattice point (RLP) at the T1–1 and T1–2 (AKANE) spectrometers. The data of the T1–1 show the spurious peak (arrow) around $h=1.09$.

tensity ratio of the Bragg peak and diffuse peak. Around the (2 0 0) Bragg-peak position, the intensity ratio of diffuse scattering peak and Bragg peak would be given by (1/4) $|(\mathbf{K}\cdot\boldsymbol{\Delta})|^2$. [$\mathbf{K}\approx\boldsymbol{\tau}(200)$]. Then, the contribution of $|(\mathbf{K}\cdot\boldsymbol{\Delta})|^2$ term in the diffuse scattering around the (1 0 0) magnetic peak can be estimated using the scattering vector $\mathbf{K}\approx\boldsymbol{\tau}(100)$. In Fig. 6(a), experimental data obtained by scanning along the [1 0 0] direction through the (1 0 0) and (2 0 0) Bragg-peak positions are given. The intensities are normalized at the Bragg-peak positions and the difference in the scattering vector $\mathbf{K}$ was taken into consideration for the diffuse scattering intensities. In the measurements of the Bragg-peak intensities, saturation of a counter was carefully avoided using the beam attenuator. As is observed in Fig. 6, the intensities of diffuse scattering are almost the same at large $\mathbf{q}$ regions but in the small $\mathbf{q}$ regions ($\mathbf{q}\lesssim 0.12$), the magnetic diffuse scattering intensity around (1 0 0) is far stronger than the nuclear diffuse scattering around (2 0 0), indicating that the extensions of the $(\mathbf{K}\cdot\boldsymbol{\Delta})\ \mathbf{S}_0^{\perp}$ term and the $\delta\mathbf{S}^{\perp}$ term are different in reciprocal-lattice space and the relation $\delta\mathbf{S}^{\perp}\gg(\mathbf{K}\cdot\boldsymbol{\Delta})\ \mathbf{S}_0^{\perp}$ is realized in the small $\mathbf{q}$ region. In this data analysis, no correction of the secondary extinction effect[12] was performed for the Bragg-peak intensities. Since the intensity of the (2 0 0) Bragg peak is far stronger than that of the (1 0 0) peak, the correction for the extinction effect leads to smaller values for the $|(\mathbf{K}\cdot\boldsymbol{\Delta})|^2$ term around (2 0 0). The similar data obtained scanning along the [1 1 0] direction at (1 1 0) are shown in Fig. 6(b).

We attempted to fit the line shape of diffuse scattering first using the Gaussian or the Lorentzian functions but it was not successful. A reasonable agreement was obtained for the squared-Lorentzian function which was derived for scattering from the macroscopic heterogeneous systems.[13] In Fig. 6, we show the best fitting curve to the experimental data for the [h 0 0] scan at (1 0 0) and the [h h 0] scan at (1 1 0). From the half width of the half maximum, the averaged inhomogeneous region is estimated to be 9.9 nm which is about 2–3 times the averaged cluster size with the lattice deformations.

Observed diffuse scattering around the (1 0 0) magnetic super-lattice point is mainly due to the modulations of the spin structure ($\delta\mathbf{S}^{\perp}$ term) coupled with the local lattice deformation. This point is also supported by following experimental data. (1) If the $(\mathbf{K}\cdot\boldsymbol{\Delta})\ \mathbf{S}_0^{\perp}$ term is far larger than the $\delta\mathbf{S}^{\perp}$ term, the distribution of diffuse scattering intensity

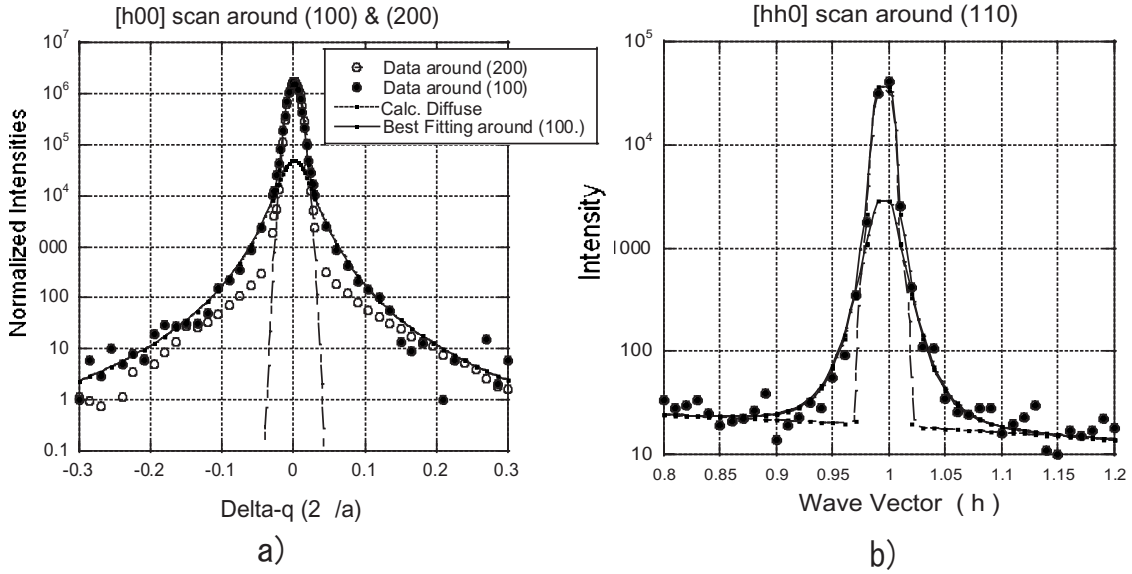

FIG. 6. (a) Diffuse scatterings studied at 10 K by scanning along the [1 0 0] direction passing through the (1 0 0) and (2 0 0) RLPs. The data were plotted in log scale and the intensities were normalized at the (1 0 0) and (2 0 0) Bragg-peak positions. Background counts were subtracted. Solid line is the best fitting curve to the line shape at (100). For the diffuse scattering, the squared Lorentzian was used. Dotted-solid line indicates Gaussian fitting to the (2 0 0) Bragg peak. (b) Line profile obtained by scanning along the [1 1 0] direction around (1 1 0) at 10 K. The Bragg peak was fitted by the Gaussian and the diffuse peak by the squared Lorentzian.

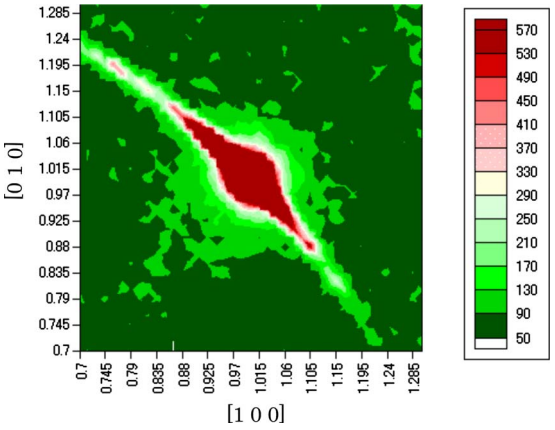

FIG. 7. (Color online) Intensity contour map of magnetic diffuse scattering obtained around the (1 1 0) super-lattice position at 10 K.

around (1 0 0) should be a butterfly pattern as is observed at (2 0 0). However, the diffuse scattering with a circular pattern is observed (except for the spurious peaks on the ⟨1 1 0⟩ axis). (2) The (1 1 0) super-lattice peak is also magnetic in origin. At (1 1 0), the $(\mathbf{K}\cdot\boldsymbol{\Delta})\,\mathbf{S}_0^{\perp}$ term would be zero along the [1 1 0] direction because the scattering vector $\mathbf{K}$ is perpendicular to the lattice displacement vector $\boldsymbol{\Delta}$. [The diffuse scattering distribution at (2 2 0) elongates only along the [1 −1 0] direction and no peak along the [1 1 0] direction (see Fig. 3 of Ref. 1).] However, the distribution of diffuse scattering observed at (1 1 0) is again circular type as shown in Fig. 7. These data show that a main contribution to the diffuse scattering at the (1 0 0) and (1 1 0) super-lattice points is the spin modulation term $(\delta\mathbf{S}^{\perp})^2$.

IV. DISCUSSIONS

It is hard to determine the actual structure of the spin modulation from the present experimental data because there are many possible ways of spin modulations under the lattice deformations such as an inclination of spin axis and a change in the magnitude of spins. The magnetic moments of Fe and Pt may behave different way. However, existence of the spin modulations coupled with the local lattice deformations would give a strong influence to the magnetism of the Invar alloys. First of all, a spin wave would be scattered by these static spin modulations, resulting in the short life time and the anomalous spin-wave damping of the Invar alloys would be explained. The fact that the high-field susceptibilities hardly saturate would also be accounted for by the spin modulations coupled with the local lattice deformations. These effects would be remarkable in low temperature because the diffuse scattering intensities around the nuclear Bragg-peak positions increased at low temperature, indicating that the amplitude of lattice distortion and the density of deformed clusters (premartensitic embryos) increased at low temperature. Then, the anomalous temperature variation in the magnetization might be explained without using the 2-γ state model. Thus, many of anomalous magnetic behaviors commonly observed in the Invar alloys would be accounted for by the spin modulations coupled with the local lattice deformations. To understand the Invar effect, importance of the coupling between the lattice deformation and the magnetism was discussed from the theoretical point of view.[14] Direct experimental evidences for these effects of the spin modulations to the anomalous magnetic behaviors will be remained as future problems.

In Fig. 6, we showed that the spin modulation term $\delta\mathbf{S}^{\perp}$ is confined to the smaller $\mathbf{q}$ region than the lattice deformation term $(\mathbf{K}\cdot\boldsymbol{\Delta})\,\mathbf{S}_0^{\perp}$. That is to say, in real space, the spin modulation extends to longer distance than the averaged radius of clusters with the local lattice deformation. This is not surprising because in deriving the Eq. (4), we assumed the localized spin model. However, for the transition-metal alloys such as the Fe_3Pt, the itinerant electrons play main role to determine the magnetic properties and the magnetic modulation would extend farther distance than the local lattice deformation.

In the present measurements, we used a nonstoichiometric alloy $Fe_{72}Pt_{28}$ to avoid the contamination of the bcc phase. Then, magnetic defect scattering would be expected because the magnetic moment of Pt is smaller than that of Fe. However, since excess Pt atoms are considered to occupy Fe cites at random, magnetic defect scattering extends over the wide space in the reciprocal lattice. Similarly, in the present measurement, we could not determine the atomic long-range order parameter of the sample because of equal scattering amplitudes of constituent atoms. Then, magnetic disorder scattering due to the wrong occupation of atoms may exist. However, the wrong occupation of atoms also takes place at random site, magnetic disorder scattering again distributes to extended space in the reciprocal lattice. Diffuse scattering confined to rather small $\mathbf{q}$ regions around the super-lattice points is considered to be due to the spin modulations around the clusters with local lattice deformation.

Apart from the spin modulations due to the local lattice deformations, Fig. 4 gives us certain information about the 2-γ state model. If we apply the 2-γ state model to the ordered Fe_3Pt alloy, reasonable numbers of Fe atoms would be excited to the low-spin state at room temperature ($T/T_c \approx 0.63$). Since the high-spin-low-spin transition is considered to take place at random Fe sites, the spin configuration at room temperature would be very similar to that of the disordered Fe_3Pt alloy with reasonably developed magnetic short-range order. Then, magnetic diffuse scattering as shown in Fig. 2 would be expected at high temperature around the (1 0 0) Bragg-peak position. Figure 8 indicates the intensity map obtained by subtraction of the 300 K data from the 10 K data. If the low-spin state increases at 300 K, negative region due to the increase in diffuse scattering has to be observed around (1 0 0). However, no indication of additional diffuse scattering at room temperature was observed. The diffuse scattering intensity at low temperature is higher than that at room temperature, suggesting that the 2-γ state model is not applicable to the ordered Fe_3Pt Invar alloys. This is consistent with the previous report of Mössbauer spectroscopy data[15] but inconsistent with the photoemission experiments.[3] Figure 8 also excludes the possibility that diffuse scattering obtained here is due to the low-energy magnon[16] which may be observed within the energy resolution of the spectrometer because the scattering intensity of magnon at room temperature should be stronger than that at the low temperature.

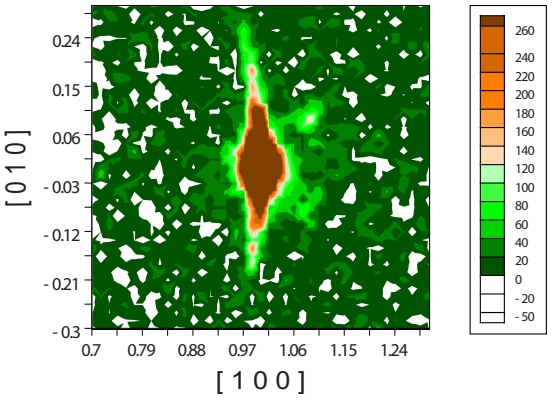

FIG. 8. (Color online) Temperature difference of the (1 0 0) intensity contour map. The data at 300 K were subtracted from those at 10 K.

V. CONCLUSION

We studied existence of the spin modulations due to the local lattice distortions in the premartensitic embryos in an ordered $Fe_{72}Pt_{28}$ Invar alloy by using neutron-scattering method. Magnetic diffuse scattering was obtained around the (1 0 0) and (1 1 0) super-lattice points. The diffuse scattering intensities increased with decreasing temperature. In the simplest approximation, magnetic diffuse scattering coupled with the lattice deformation consists of two components; the lattice displacement of the localized spins and the modulation of spin structure due to the lattice deformation. Present experimental data showed that spatial extensions of these two components are different and the latter extends to longer distance ($\sim$10 nm) than the former and the scattering intensity of the latter is far stronger than that of the former.

Unfortunately, actual spin structure of spin modulation could not be determined from the present experiments but existence of spin modulations is considered to have important influences to the static and dynamical magnetic properties of the Invar alloys. Many of anomalous magnetic behaviors as common properties of the Invar alloys reported by previous authors would be explained by the spin modulations coupled with the local lattice deformations in the clusters which are formed as a premartensitic phenomenon of the fcc-bcc martensitic phase transition.

ACKNOWLEDGMENTS

We thank K. Ohyama (Tohoku University) for giving us a chance to use the T1-2 (AKANE) triple-axis spectrometer for checking multiple scattering.

[1] Y. Tsunoda, L. Hao, S. Shimomura, F. Ye, J. L. Robertson, and J. Fernandez-Baca, Phys. Rev. B **78**, 094105 (2008).
[2] R. J. Weiss, Proc. Phys. Soc. London **82**, 281 (1963)
[3] E. F. Wasserman, in *Ferromagnetic Materials*, edited by K. H. J. Buschow and E. P. Wahlfarth (North-Holland, Amsterdam, 1990), Vol. 5, pp. 237–322.
[4] O. Yamada, F. Ono, I. Nakai, H. Maruyama, F. Arae, and K. Ohta, Solid State Commun. **42**, 473 (1982).
[5] F. Ono and S. Chikazumi, J. Phys. Soc. Jpn. **37**, 631 (1974).
[6] Y. Ishikawa, Y. Noda, K. R. A. Ziebeck, and D. Givord, Solid State Commun. **57**, 531 (1986).
[7] Y. Ishikawa, S. Onodera, and K. Tajima, J. Magn. Magn. Mater. **10**, 183 (1979).
[8] Y. Ishikawa, M. Kohgi, S. Onodera, B. H. Grier, and G. Shirane, Solid State Commun. **57**, 535 (1986).
[9] L. Nataf, F. Decremps, M. Gauthier, and B. Canny, Phys. Rev. B **74**, 184422 (2006); M. Matsushita, T. Inoue, I. Yoshimi, T. Kawamura, Y. Kono, T. Irifune, T. Kikegawa, and F. Ono, *ibid.* **77**, 064429 (2008).
[10] P. Entel, E. Hoffmann, P. Mohn, K. Schwarz, and V. L. Moruzzi, Phys. Rev. B **47**, 8706 (1993).
[11] M. van Schilfgaarde, I. A. Abrikosov and B. Johansson, Nature **400**, 46 (1999).
[12] For a sample with narrow mosaic spread, incident neutrons would be scattered by the surface area of the sample and would not attain the deep inside of the sample. Then, the scattering intensity is not proportional to the sample volume. This effect is rather severe problem for the Bragg peak with strong intensity but is not easy to carry out the correction.
[13] P. Debye and H. R. Anderson, Jr., and H. Brumberger J. Appl. Phys. **28**, 679 (1957).
[14] S. Lipinski and M. Pugaczowa-Michalska, Physica B (Amsterdam) **269**, 227 (1999).
[15] K. Sumiyama, M. Shiga, K. Tachi, and Y. Nakamura, J. Phys. Soc. Jpn. **40**, 1002 (1976).
[16] Y. Ishikawa, K. Tajima, Y. Noda, and N. Wakabayashi, J. Phys. Soc. Jpn. **48**, 1097 (1980).